Computers & Graphics xxx (xxxx) xxx

Contents lists available at ScienceDirect

Computers & Graphics

journal homepage: www.elsevier.com/locate/cag

Special Section on Adv Graphics+Interaction

Microstructure-based appearance rendering for feathers

Jessica Baron *, Daljit Singh Dhillon, N. Adam Smith, Eric Patterson

Clemson University, 1240 Supply Street, North Charleston, SC, 29405, USA

ARTICLE INFO

Article history:
Received 28 July 2021
Received in revised form 19 September 2021
Accepted 24 September 2021
Available online xxxx

Keywords:
Computers and graphics
Appearance modeling
Biological modeling
Natural phenomena
Reflectance
Shading models

ABSTRACT

The appearance of a real-world feather is the result of light interactions with complex, patterned structures of varying scale; however, these have not yet been modeled for accurate rendering of feathers in computer graphics. Previously published works related to production and research have presented simplified curve models to represent the appearance of feathers. In this work we present why these approaches are not sufficient using imaging from real feathers along with motivation for a specific appearance model for feathers. We also propose and compare a new technique that takes into account the detailed substructures of feathers and their role in rendering an accurate far-field appearance. Our proposed method lends a high degree of photorealism for rendering feathers in visual-effects and content-creation applications.

© 2021 Elsevier Ltd. All rights reserved.

Fig. 1. An osprey feather photographed (left portion) and modeled as curves and rendered as hair fibers (middle) and with simulated microstructures (right).

1. Introduction

Bird feathers are a complex assembly of multi-scale structures including the central shaft, branching barbs, and interlocking barbules on those barbs. This hierarchical structure provides a variety of unique functions for the feathered organism such as flight and display, the latter based on coloration where each component of a feather contributes to the overall appearance. In many feathers this coloration is due to pigmentation from carotenoids (yielding yellows and oranges), melanins (yielding browns and blacks), and porphyrins (yielding browns, reds, and greens and which can fluoresce reds under ultraviolet light). Some feathers additionally or primarily exhibit structural coloration due to melanosome patterns at a nanoscale level, leading to iridescence, bright blues or combinations of colors in conjunction with pigmentation [1,2]. Apart from coloration, the optical properties and structures produce a variety of intriguing effects such as glow, shine, and highlights that depend on the surrounding lighting.

Although extensive work has been done in representing real-world objects by material models for computer graphics, a physically based model for accurately representing the light-surface interactions of feathers has not yet been presented. Such an appearance model would eventually need to include an accurate wave-optics model to describe structural coloration effects. We suggest that ahead of that, though, a more fundamental model is a first step to represent the diffuse and specular reflectances of this complex assembly of multiple scales.

At some level one of the most important aspects of such an improved material model is to represent the aggregate effect of feather micro- and nanoscale substructures when viewed from a distance. These multi-scale effects are not considered in current renders of feathers as geometry is usually simplified to the shaft and barbs only, representing the barbs with either Non-uniform Rational B-Splines (NURBS) or Bézier curves. Fiber-scattering models developed primarily for representing hair have been the shading model typically chosen to render these curves [3–6]. We suggest and demonstrate that a collection of curves representing feather barbs but not the smaller structures lacks significant components needed for photo-realism. We also suggest that the Bidirectional Curve Scattering Distribution Functions (BCSDFs) typically used for shading hair and fur do not likely well represent light scattering of feather substructures due to their unique shapes.

The structure of this paper includes a brief summary of related work for rendering natural materials; information on the

* Corresponding author.
E-mail addresses: jrbaron@clemson.edu (J. Baron), djsingh@clemson.edu (D.S. Dhillon), smith23@clemson.edu (N.A. Smith), ekp@clemson.edu (E. Patterson).

https://doi.org/10.1016/j.cag.2021.09.010
0097-8493/© 2021 Elsevier Ltd. All rights reserved.

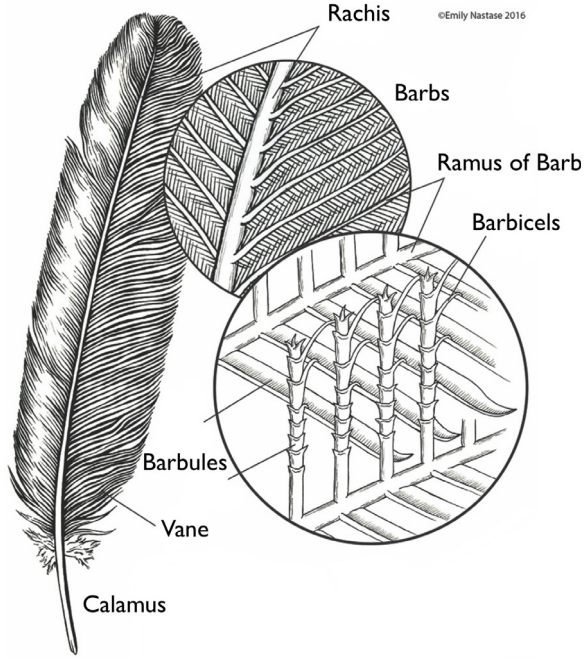

Fig. 2. Illustration of feather structure.
Source: Modified from [7].

fundamental aspects of feathers that affect their appearance; motivation for a specific shading model for feathers; presentation of a new method aimed at representing some of the appearance properties due to the multi-scale scattering effects of feathers; and suggestions for future work.

In summary, the primary contributions of this paper are:

1. Evidence and discussion presenting a strong motivation for development of specific shading models for feathers.
2. Presentation of research questions and possible approaches.
3. The introduction of a new technique capable of representing key far-field appearance properties arising from achromatic scattering by the multi-scale components of feathers.

2. Background

A variety of models have been suggested for various materials as the discipline of computer graphics has progressed. Some of these include simple diffuse-specular models, more complex subsurface-scattering models, and even multi-scale and layered-material models. Microstructure cylindrical models have particularly been developed for rendering hair, fur, and cloth fibers. We present here a summary of physically based material models that could be considered similar in some ways to components of feathers followed by a brief description of the structure and coloration of physical feathers.

2.1. Physically based rendering and materials

A material is usually simulated by a Bidirectional Reflectance Distribution Function (BRDF) where there have been many functions proposed for a large variety of real-world and synthetic materials. BRDF terminology and measurement standards were introduced in [8]. The development of physically based material models stems from studies on geometric optics, namely the Torrance–Sparrow microfacet model [9] later adapted for use in physically based rendering for computer graphics by Cook and Torrance [10] and expanded to represent both reflection and transmission as a Bidirectional Scattering Distribution Function (BSDF), now a common standard in physically based rendering [11]. Additional variations of appearance models including subsurface-scattering [12,13], multi-scale [14], layering [15,16], and diffractive and iridescent models [17–19] are of inspiration for the continued development of a physically accurate feather model.

Bidirectional Fiber (BFSDFs) or Curve (BCSDFs) Scattering Distribution Functions represent parametric curves as cylinders or shapes enclosed by cylinders rather than mesh surfaces, making their use more appropriate for rendering filaments such as cloth and hair fibers [20,21]. These models often have both near-field representations of light scattering through the fiber using the BFSDF and far-field approximations based on distant light sources and viewing using the BCSDF [20]. Variations to hair models include azimuthal scattering with elliptical rather than circular cross sections [22] and increased efficiency using spherical harmonics [23]. Yan et al. proposes a variation for animal fur involving additional scattering based on a more prominent medulla within the fibers [24]. The reference technique covered in this paper focuses on the Marschner BCSDF [21] which is discussed more in Section 3.1 as it has been applied to production [25–27] and often been used in feather rendering to date [3,4,28]. We emphasize that the current state of the art methods do not accommodate for multi-scale structural variations in feathers.

2.2. Feather structure and coloration

Here we present related material from ornithology, the study of birds, covering the hierarchical feather structure, nanoscopic composition, and pigmented and structural coloration.

A feather is a hierarchical structure of branching components that is illustrated in Fig. 2. The structure has a central *shaft* and two *vanes* (posterior and anterior). Vanes are composed of hundreds of adjacent *barbs* each of which consists of many *barbules* extending from a *ramus* (plural *rami*). These barbules possess *pennulae* which act as hooks (called *barbicels* on the *distal barbules*) and rods (on the *proximal barbules*) to form the surfaces of the vanes. Feather structure serves a wide variety of functions such as flight, insulation, water repellency, and visual signaling [29–31]. A feather is composed of the protein keratin of which human hair and nails are also composed. The coloration of feathers is pigmented, structural, or combinations of the two. Pigmented colors are caused by components such as melanin-producing melanosomes and carotenoids from food sources [2,32], and structural coloration occurs based on nanoscale arrangement and orientation of melanosome, keratin, and air layers [33,34].

Case studies of feather coloration, including iridescent effects, are found in ornithological research investigating avian visual signaling and sexual selection [35–40]. Paleontologists actively research the coloration of extinct dinosaur feathers based on the micro- and nanoscale arrangements found in fossilized specimens compared to those in feathers of extant birds [41–44]. Structural coloration effects are beyond the scope of our current work. However, there are important appearance effects to begin to model for improved fidelity of renders.

3. Related work

This section reviews particularly related work in material modeling and the previous publications related to computer-generated feathers.

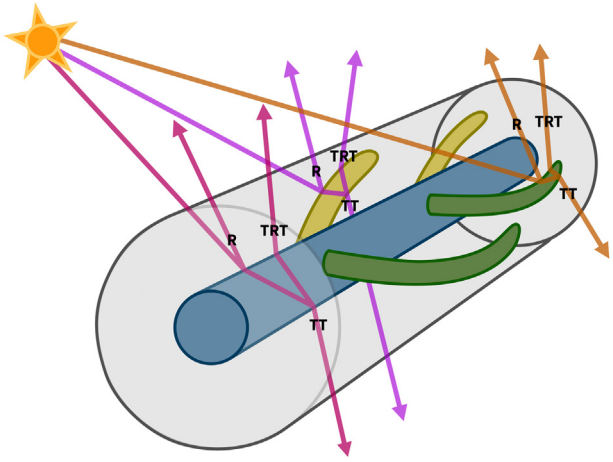

Fig. 3. Light-transport paths summarizing the proposed feather-shading technique. Specular lobe paths scatter on the ramus (red path, blue shape), proximal barbule (purple path, yellow shape), and distal barbule (orange path, green shape) within a section of the curve defining the entire barb. The R, TT, and TRT path labels describe reflection and transmission according to [21]. (For interpretation of the references to color in this figure legend, the reader is referred to the web version of this article.)

3.1. Material capture and modeling

Many physically based material models have been derived through fitting analytical functions to or storing look-up tables of measured reflectance data. We consider three main categories of material models relevant when studying feathers: fiber, iridescent, and multi-scale models.

Fiber, hair, or BCSDFs in general model scattering along the length and width of a cylindrical structure following the path of a curve segment. The widely adopted and expanded Marschner-hair model was developed by observing cuticles on round hairs using electron-microscope images [21]. The far-field reflectance was measured with image-based techniques, and a BCSDF was used to model transmission and reflectance paths. The Marschner model has been adopted widely in film and game production [25–27,45,46].

Recent material research also includes investigation of spectrally dependent effects such as diffraction exhibited by natural phenomena like snakeskins [18] and thin-film iridescence [19]. Material models have been developed for multi-scale light reflectance based on milli- and microgeometry [14], for scattering in volumetric layers of materials [47], and based on approximations of X-ray microtomography (micro-CT) of fabrics [48].

3.2. Feathers in computer graphics

Chen et al. procedurally modeled feathers based on control Bézier curves and textured them with a Bidirectional Texture Function (BTF) [49]. The BTF was presented for describing materials as textures based on lighting and viewing directions [50]. Baron and Patterson focused on the procedural generation of more detailed feather geometry based on image analysis of photographed feathers and including barbule curves in addition to the shaft and barb curves [51].

Hair models are pertinent due to their wide use in production for shading computer-generated feathers. For near-field reflectance, feathers are often modeled only to the barb level as a series of hair curves [3,4,28]. Geometry cards have been used in rendering feathers distant from the camera, and there may be other level-of-detail representations between near field and far field implemented [52]. Some other work has been presented on feather system "grooms" and simulated animation but is not pertinent here for appearance modeling.

The ornithological investigations of Harvey in [35,53] were not aimed at computer graphics but focused on methods to study the reflectance of a prominently iridescent bird species in terms of avian visual signaling for mating. This work did not present a scattering model for feathers but raised an important idea that we build upon; the distal barbules, pennulae, and proximal barbules, particularly the pennulae, contribute significant reflected radiance. See section 5.2.1. and 5.2.2 in [35] for further details on their observations regarding percentage of reflected radiance. This is compared to radiance reflected by the central ramus of a barb which is the only structure represented by a curve with a BCSDF such as in nearly all published feather-related work to date.

Inspired by the works presented in this section, we propose a substructure-based method of representing the multi-scale light interactions with different portions of the feather-structure hierarchy, illustrated by Fig. 3.

4. Motivation for feather-specific shading

As noted, feather substructures do significantly affect the far-field appearance of the entire feather. The only known prior work that observes these structures of feathers from the context of both ornithology (visual signaling) and information useful for material modeling (optical measurements and plotting) is in [35,53].

As described in [35], interactions of light with feathers' unique surfaces occur at the organism-, macro-, milli-, micro-, and nanoscales, and the orientation of microstructures and arrangements of the nanoscale components drive the resulting appearance. Macroscale reflectance concerns patches of feathers. A feather's shaft and vanes are at the macroscale where the vanes appear flat. The barbules and rami of barbs compose the prominent milli- and microscale details. The distal and proximal barbules of adjacent barbs interlock via their pennulae respectively acting as hooks and rods. Diffraction at the nanoscale produces structural coloration. The measurements and observations in [35,53] demonstrate that light reflecting off of the milli- and microscale feather substructures contribute to the majority of feather's far-field appearance.

Feathers and hair differ distinctly in micro- and nanostructures. Fig. 4 displays human hairs next to non-iridescent wing feathers of a Rock Dove, both imaged with a Scanning Electron Microscope (SEM). These structures differ significantly from one another and should be expected to reflect light differently. Nanoscopic imagery using Transmission Electron Microscopy (TEM) reveals sub-wavelength layers and pockets of melanosomes, keratin, and air that can cause wave interference and structural coloration in addition to pigmented color [33,34]. Human hair also has micro- and nanoscopic arrangements of melanosomes although these are distributed within the cortex of the hair rather than in complex, layered arrangements as found in feathers [54].

The main question addressed in this paper is: Is some representation of feather microstructures needed qualitatively for more photorealistic feather rendering? We emphasize the idea that the substructures, particularly the barbules and their pennulae, contribute significantly to the far-field appearance of feathers, and therefore, sampling current BSDFs or BCSDFs does not produce a high-fidelity appearance. We investigate modeling the reflectance of these important components with a substructure-based technique in this work.

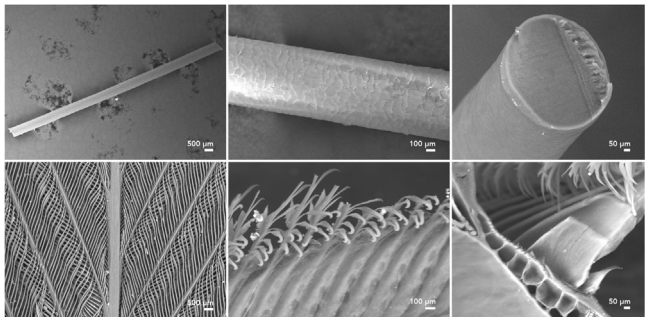

Fig. 4. Scanning-electron microscope (SEM) images taken by the authors. Top row: Human hair at varying scales and cross section. Bottom row: Feather shaft, barb, and barbule structures; barbule edges; and barb cross section. Note the complex layered structure of feathers as well as significant differences in shape and internal composition of a barb cross section versus a hair cross section.

Fig. 5. Sample of photographs captured with the dome under varying illumination. Note the changes in specular highlights on the microstructures.

5. Proposed method

This section presents a new technique in approximating micro-geometry, introduces different tests concerning shading and rendering to represent light scattering on feather components, covers preparing geometry for rendering, and discusses the environment for rendering and development. Section 6 compares the renders resulting from different rendering approaches against photographs of real feathers.

5.1. Preparation

Several feather specimens were photographed in a controlled lighting environment for comparison, including the wing covert of an osprey depicted in Fig. 5. The capture environment is a variable-lighting hemisphere equipped with 25 white LED lights and custom software for controlling light combinations. The photographs capture the specular highlights of the feather's various barbules and rami due to changes in the incident illumination. Note that feather structure was not captured using photogrammetry and structured light because these approaches cannot reconstruct the fine substructures; also, in multi-view stereo captures, some knowledge of the shading model is essential which is yet unknown and a focus of this study. The photographs primarily serve as reference images for qualitative comparison in this study.

Microscopic images of feather specimens were also taken, and Fig. 6 consists of more SEM images of a Rock Dove feather. The left image includes several adjacent views from the dorsal (externally facing, away from the body) side of the feather; the top shows the ventral (opposite of dorsal) side of a single barb (based on the hooklets curling towards the sensor); and the bottom shows the cross sections of the shaft and adjacent barbs and their rami facing towards the calamus or base of the feather. These images provide insight into the substructure arrangement that inspired the technique presented here.

We created synthetic versions of the osprey feather along with a Turkey Vulture back-covert feather and a Rock Dove wing feather based on an implementation of the procedural-geometry generation presented in [51]. Models from this approach are composed of a series of B-spline curves with one central curve representing the shaft and many adjacent branching curves for the barbs. Note that these curve-based models do not precisely match the real specimens in number of barbs due to limitations in capturing fine structures. The geometric models are placed in a virtual scene with a simulated dome matching the real-world lighting hemisphere, lighting in a similar manner to the photographed conditions.

5.2. Shading and rendering

In this paper we compare two different approaches of representing the far-field light scattering of feathers: rendering the shaft with barb curves only using a hair model as has been done typically elsewhere and rendering the shaft as hair and the barbs with a proposed substructure-based technique that simulates the barbules and rami. (The choice of using a hair BCSDF for the substructures and addressing its limitations is explained in Section 5.4.)

The first approach to shading the feather involves a direct application of the Marschner hair model to the geometric representation of barbs alone as cylindrical fibers, and it serves as the reference point for comparing improvements arising from the proposed substructure-based method. A projected texture of low-frequency albedo based on an image taken under diffuse, cross-polarized conditions in the lighting dome is used to drive the model's coloration.

The proposed substructure-based technique takes the same barbs-only, geometric model as in the first approach. However, it incorporates the effects of microscopic geometry for barbules that lie within the outer simplified cylindrical representation for a given barb. This is explained further in Section 5.3.

Explicitly creating barbule geometry could be closer to visual fidelity, and including barbules by some method is still significant. That level of micro-geometry even simplified is very expensive to handle, though; hundreds or thousands of curves, times hundreds or thousands more, even instanced, may not be desired.

5.3. The proposed substructure-based technique

In general the proposed technique performs two steps at shading evaluations. At first, we traverse the feather geometry to determine the locations of simplified substructure shapes. Next, we shade the located substructure shapes as individual fibers. This approach is physically inspired by the presence of feather substructures but is a simplification of both the arrangement and reflectance of those substructures. We describe this approach as a shading "technique" because we do not yet present a fully developed scattering model for feather-light interactions.

Feather Geometry Traversal: For the given shading location, within the shader program, we first traverse the feather geometry to determine the structural element being sampled through the

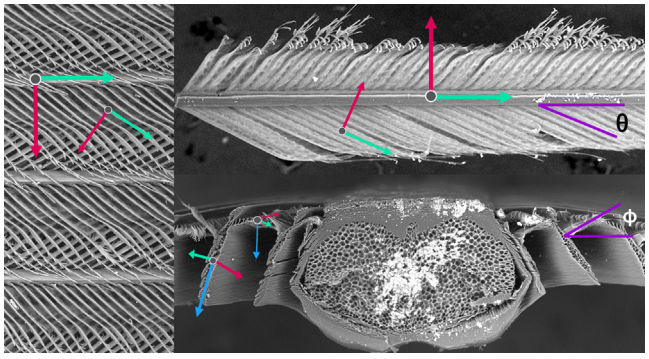

Fig. 6. SEM images of a Rock Dove feather. Left: Interlocked barbs (dorsal view) spanning about 4 mm horizontally. Top: Section of a single barb (ventral view) about 11 mm wide. Bottom: Cross section of shaft and barbs about 20 mm wide. Conventions used in this work are illustrated over the SEM captures: barbule elevation and azimuth (purple angles), barb orientation (larger axes), barbule orientation (smaller axes). Green indicates the tangent, red the bitangent, and blue the normal. (For interpretation of the references to color in this figure legend, the reader is referred to the web version of this article.)

pixel being rendered. As discussed in Section 2, a single barb contains a central ramus and proximal and distal barbules branching from the ramus (see Fig. 2). Fig. 6 depicts these structures with SEM images and labels for angles and local axes, and this convention is applied to the proposed shading technique. Similar notation is used for describing ramus and barbule shading frames as indicated by the pairs of larger (ramus) and smaller (barbule) axes drawn in Fig. 6. Instead of explicitly defining geometry, the proposed technique uses the parametric coordinates of points sampled with path tracing along the cylindrical curve that bounds a single barb of a feather. The parametric coordinates determine which micro-structure (distal barbule, proximal barbule, or ramus) is sampled, and the sampled curve orientation is modified accordingly for shading.

The local positions and transformations of the ramus and proximal and distal barbules within a barb are computed first. If the point currently sampled on the barb curve also lies on the ramus of the barb, it assumes the same eccentricity as defined for the entire barb curve and is sampled using the curve tangent $\hat{t}$, normal $\hat{n}$, and bitangent $\hat{b}$. If the point is located within the periodically defined areas of the barbules, that portion of the curve is shaded using an altered orientation with barbule tangent $\hat{t}_b$, normal $\hat{n}_b$, and bitangent $\hat{n}_b$ which vary on whether the barbule is distal or proximal. If the sampled point is neither a part of a barbule or the ramus, it is evaluated as pure transparency, say T. We choose to treat the ramus and barbules as cylindrical hair fibers in our method. This simplification along with other approximations devised in our method are discussed further in the next subsection, 5.4.

The placement and orientation of substructures can be controlled through user defined parameters for the ramus and barbule radii, barbule elevation θ_b (rotation away from barb tangent), barbule azimuth ϕ_b (lift away from vane using the barb bitangent), and a flag indicating whether a barb belongs to the left or right vane of a feather. The angles discussed here are illustrated over the SEM images in Fig. 6. A ramus-barbule geometric term, $G_b(u, v, \hat{n}_b, \hat{t}_b)$ is computed based these user-defined attributes, the parametric (u, v) coordinates of the sampled point along the barb curve, and the corresponding orientation to determine if the point lies on a ramus, barbule, or neither; see Algorithm 1 for details. Restrictions on (u, v) are based on where the ramus lies centered along curve's width (between bounds $u0$ and $u1$ where for a barbule $u \in [0, u0] \cup [u1, 1]$) and the portion of the curve's length where the barbule base connects to the ramus between bounds $v0_{base}$ and $v1_{base}$. A barbule direction from base to tip and the distance the sampled point is along the barb are found and used for determining the exact restriction on v (where $v \in [v0, v1]$).

Data: num barbules per vane N; barbule and ramus radii r_b, r_r; barb orientation $\hat{t}$, $\hat{n}$, $\hat{b}$; barbule angles θ_b, ϕ_b; flag *whichVane*
Result: flags *isBarbule*, *isRamus*, *isDistal*

isRamus = *isBarbule* = *isDistal* = False;
Find bounds $u0$, $u1$ along curve width;
Set *isDistal* using *whichVane* and u;

if $u <= u0$ *or* $u1 <= u$ **then**
  $\hat{t}_b$ = BarbuleOrientation($\hat{t}$, $\hat{n}$, $\hat{b}$, θ_b, ϕ_b, *isDistal*);
  Find bounds $v0$, $v1$ along curve length using distance along barbule;
  if $v0 <= v$ *and* $v <= v1$ **then**
    isBarbule = True;
  end
end
else
  isRamus = True;
end

Algorithm 1: Ramus-barbule geometric term $G_b(u, v, \hat{n}_b, \hat{t}_b)$ determining the locations of barb substructures and using the barbule-orientation function in Algorithm 2.

Algorithm 2 computes the barbule orientation $\hat{t}_b$, $\hat{n}_b$, $\hat{b}_b$ based on the barb's orientation and barbule angles θ_b, ϕ_b. These axes are altered if the barbule is distal to simulate the curve of the tip with hooks, rotating $\hat{t}_b$ about $\hat{n}$ based on how far away the sampled point is along the hooked tip of the barbule (pennula). Using the geometric information deduced from this traversal step, our next step performs substructure shading.

Data: $\hat{t}$, $\hat{n}$, $\hat{b}$, θ_b, ϕ_b, *isDistal*
Result: $\hat{t}_b$, $\hat{n}_b$, $\hat{b}_b$

$\hat{t}_b$ = Rotate $\hat{t}$ about $\hat{n}$ by θ_b then about $\hat{b}$ by ϕ_b;
$\hat{b}_b = \hat{n} \times \hat{t}_b$;
$\hat{n}_b = \hat{t}_b \times \hat{b}_b$;

if *isDistal == True* **then**
  $\theta_{hook} = t * \frac{\pi}{2}$ where t is distance along hooked portion of barbule;
  $\hat{t}_b$ = Rotate $\hat{t}_b$ about $\hat{n}$ by θ_{hook};
end

Algorithm 2: Barbule-orientation function for determining the new tangent, normal, and bitangent of a barbule.

Substructure Shading: The above traversal step clearly establishes the shape, location, and orientation of the substructure being sampled. The radiance returned during shading is now calculated as if each substructure were a unique fiber to sample. Eq. (1) describes the substructure-based technique $S_B(\theta_i, \phi_i; \theta_r, \phi_r)$ (S for "scattering" and B for "barb") based on the Marschner hair-scattering model (denoted here with H for "hair") $S_H(\theta_i, \phi_i; \theta_r, \phi_r)$ and driven by a ramus-barbule geometric term $G_b(u, v, \hat{n}_b, \hat{t}_b)$ summarized in Algorithms 1 and 2 and illustrated in Fig. 3.

$$S_B(\theta_i, \phi_i; \theta_r, \phi_r) = \begin{cases} S_H(\theta_i, \phi_i, \theta_r, \phi_r | \hat{t}, \hat{n}, \hat{b}) & isRamus \\ S_H(\theta_i, \phi_i, \theta_r, \phi_r | \hat{t}_b, \hat{n}_b, \hat{b}_b) & isBarbule \\ T(\theta_i, \phi_i, \theta_r, \phi_r | \eta = 1) & otherwise \end{cases} \quad (1)$$

The Marschner model S_H describes the hair scattering in terms of longitudinal and azimuthal scattering for the reflection (R), transmission (TT), and transmission–reflection (TRT) specular lobes based on the incident and reflected directions (θ_i, ϕ_i) and (θ_r, ϕ_r)

Fig. 7. Turkey Vulture feather photographed (left) and rendered (right) with the left vane using the substructure-based technique and the right vane as hair.

along with a tilt of the overlapping scales on a hair's surface and an eccentricity describing the shape of its cross section [21]. Using Eq. (1), we achieve final shading through an on-the-fly, substructure adapted realization of the Marschner model for scattering or by entirely skipping it for a transmission path.

5.4. Justification of simplifications

This technique is a fundamental approach to developing a feather-specific shader. The Marschner hair-shading model was chosen as a basis due to its common use in the production industry for attempting to render photorealistic feathers, that implementations and variations are readily available, and that the model is well understood by many. The Marschner BCSDF, of course, models circular cross-sections like hair. The shape of the ramus, though, differs greatly and thus its reflectance and transmittance likely are not well modeled by a BCSDF, including even more recent fiber models that model larger eccentricity. (Note the unique, elongated shape of the rami cross sections in the bottom image of Fig. 6.) The shaft cross section of a more elliptical shape is in the center of this image. As a readily available implementation, though, and an efficient model on which to base this initial work, a Marschner-like model across the various scales of the structures of feathers could possibly generate similar far-field effects to those desired. Additional simplifications are taken in both the curve-based geometric representation of barbule shape and also in the periodic-based simulation in the presented method. Although additional physical data collection could provide insight, we demonstrate in the results section that the proposed approach already produces a high degree of photo-realism versus the current state-of-the-art.

5.5. Rendering and development environment

Pixar Animation Studio's RenderMan [55] is used here for rendering. The new architecture since RenderMan 21 is path traced and provides a "BxDF" (Bidirectional *x* Distribution Function) interface for introducing new material models. We use this interface along with the included hair implementations and RenderMan for Maya plug-in.

The barb and barbule curves of the feather geometry rendered as hair use the PxrMarschnerHair BxDF. The implementation of this material is described in a Pixar Technical Memo [26]. The substructure-based technique is implemented as a custom RenderMan BxDF. More specifically, it is a variation of PxrHair, a simplified version of PxrMarschnerHair publicly available with the RenderMan source code Examples.

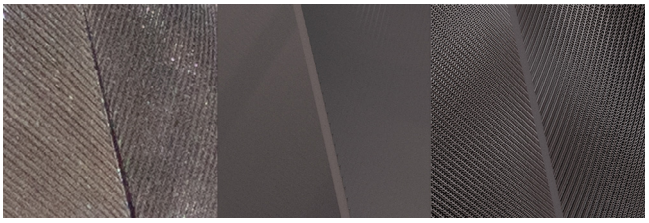

Fig. 8. Portion of Rock Dove feather photographed (left), modeled and rendered with curves as hair (middle) and with curves simulating barbules and rami using the proposed substructure-based technique (right).

6. Results

6.1. Comparisons

Fig. 1 shows portions of the osprey feather as the original photograph with all dome lights on (left) and the model of barb curves rendered as hair fibers (middle) and with the proposed BCSDF simulating rami and distal and proximal barbs and barbules (right). Note the variation in specularity in the original that the middle hair-fiber approach does not represent, but the proposed method demonstrates at least partially.

Fig. 7 displays a photograph (left) of a Turkey Vulture back feather and a corresponding rendered model (right) where the left vane is shaded using the substructure-based technique and the right vane as hair fibers. Fig. 8 compares a portion of a photograph of a Rock Dove wing feather with two rendered versions using a hair model and the proposed method. For both feathers the same curve width parameter was used for the hair and substructure versions. The proposed substructure-based method creates far-field glints more similar to those captured in the photographs.

6.2. Discussion, limitations, and future work

We show that representing light reflected from the substructures of feathers is significant in achieving photo-realistic renders of synthesized feathers. Although the approach of treating feather barbs as individual hair fibers has been used throughout production, a simple hair model does not accurately describe the far-field reflectance of a feather due to the specularity of the barbules and rami of barbs as shown in Figs. 1, 7, and 8. This is due to a large portion of reflected radiance originating from the barbules, and current BCSDF approaches do not represent such substructures.

The renders synthesized with the new technique reach a greater photo fidelity than barb-curve renders alone, even with a cylindrical BCSDF that is an overly basic approximation to the underlying micro-structure shapes.

Like many existing BxDF models (e.g. [9,11–13,17,18,21]), our method does not explicitly evaluate multi-scale rendering effects. Also, we do not explicitly model interactions across multiple substructures within a barb. A light transport framework for modeling global illumination should however be able to accommodate these limitations with adequate sampling either directly or through simple adaptations; this would be a direction of future research.

At a much broader level and after this initial investigation addressing the need for representing feather micro-structures, we present several key research questions related to developing a full feather appearance model.

1. Could using a different BCSDF such as one that includes more eccentricity/azimuthal scattering get closer? (This is unlikely since it does not represent the large percentage of far-field reflectance contributed by the distal barbules, pennulae, and proximal barbules.)
2. Could we represent the missing components in a BTF-like model representative of the substructures?
3. Would (3) be better done using barbule curves in simple or more advanced shapes along with a BCSDF? And if so, what type of BCSDF would give best results? Are models with more complex azimuthal scattering better and by how much?
4. How would a full geometric representation of distal barbules, pennulae, and proximal barbules compare to the approaches above?
5. What is the compared efficiency of different approaches? What are the best approaches for various applications and why?

Each of these open research questions serve an interesting direction for future work.

7. Conclusions

We conclude that the curves rendered using the proposed substructure-based method reach greater photo-fidelity versus using a hair model on individual barb curves as has been typically done so far; this is due to the total light scattered from the substructures that make up a single barb contributing to the overall appearance. Rendering these microstructures without explicitly modeling them represents a fundamental improvement in the non-structural-color rendering of feathers and a basis that will serve for future investigations, particularly concerning structural coloration and wave interference.

In future work we seek to include a wider variety of feathers, a more elaborate scattering distribution term that matches the non-cylindrical shapes shown by SEM, improved models for each feather component, a far-field aggregated BSDF, and wave-optics models for both blues and iridescent responses, also with varying effective viewing angles to adapt the proposed method for a larger variety of feathers.

Lastly, creating a fully detailed geometric representation of distal barbules, pennulae, and proximal barbules could be useful for testing and evaluating future models. This might be achieved with the aid of volumetric micro-CT scans.

CRediT authorship contribution statement

Jessica Baron: Software, Conceptualization, Methodology, Data curation, Writing – original draft, Visualization, Funding acquisition. **Daljit Singh Dhillon:** Writing – review & editing, Validation, Funding acquisition. **N. Adam Smith:** Ornithological oversight, Resources, Funding acquisition. **Eric Patterson:** Supervision, Conceptualization, Data curation, Writing – original draft, Project administration, Funding acquisition.

Declaration of competing interest

Clemson University

Acknowledgments

We would like to thank the Carolina Raptor Center for feather specimens and Ubisoft Red Storm for the variable lighting hemisphere.

This material is based upon work supported by the National Science Foundation under Grant No. 2007974.

References

[1] Martyniuk MP. A field guide to Mesozoic birds and other winged dinosaurs. Pan Aves; 2012.
[2] How birds make colorful feathers. 2015, https://academy.allaboutbirds.org/how-birds-make-colorful-feathers/ [Accessed 7 April 2020].
[3] Leaning J, Fagnou D. Feathers for mystical creatures: Creating pegasus for clash of the titans. In: ACM SIGGRAPH 2010 Talks. New York, NY, USA: ACM; 2010, http://dx.doi.org/10.1145/1837026.1837094, 52:1–52:1.
[4] Crow T, Hoffman J, Lee M, Poh K. Shading dory's new friends. In: ACM SIGGRAPH 2016 Talks. New York, NY, USA: ACM; 2016, http://dx.doi.org/10.1145/2897839.2927440, 76:1–76:2.
[5] Frei V. Maleficent – mistress of evil: Jessica norman – VFX supervisor – MPC. 2019, Art of VFX.
[6] McGowan C. Balancing photorealism and animal personality in dolittle. VFX Voice - the Magazine of the Visual Effects Society 2020.
[7] Nastase E. Pennaceous feather structure. 2016, http://www.emilynastase.com/fauna/ [Accessed 1 August 2018].
[8] Nicodemus F, Richmond J, Hsia J, Ginsberg IW, Limperis T. Geometrical considerations and nomenclature for reflectance. 1977.
[9] Torrance K, Sparrow E. Theory for off-specular reflection from roughened surfaces ∗. J Opt Soc Amer 1967;57(9):1105–14. http://dx.doi.org/10.1364/JOSA.57.001105, URL http://www.osapublishing.org/abstract.cfm?URI=josa-57-9-1105.
[10] Cook R, Torrance K. A reflectance model for computer graphics. ACM Trans Graph 1982;1(1):7–24. http://dx.doi.org/10.1145/357290.357293.
[11] Walter B, Marschner SR, Li H, Torrance KE. Microfacet models for refraction through rough surfaces. In: Proceedings of the 18th eurographics conference on rendering techniques. Goslar, DEU: Eurographics Association; 2007, p. 195–206.
[12] Hanrahan P, Krueger W. Reflection from layered surfaces due to subsurface scattering. In: Proceedings of the 20th annual conference on computer graphics and interactive techniques. New York, NY, USA: Association for Computing Machinery; 1993, p. 165–74. http://dx.doi.org/10.1145/166117.166139.
[13] Jensen HW, Marschner SR, Levoy M, Hanrahan P. A practical model for subsurface light transport. In: Proceedings of the 28th annual conference on computer graphics and interactive techniques. New York, NY, USA: Association for Computing Machinery; 2001, p. 511–8. http://dx.doi.org/10.1145/383259.383319.
[14] Westin SH, Arvo JR, Torrance KE. Predicting reflectance functions from complex surfaces. In: Proceedings of the 19th annual conference on computer graphics and interactive techniques. New York, NY, USA: Association for Computing Machinery; 1992, p. 255–64. http://dx.doi.org/10.1145/133994.134075.
[15] Weidlich A, Wilkie A. Arbitrarily layered micro-facet surfaces. In: Proceedings of the 5th international conference on computer graphics and interactive techniques in Australia and Southeast Asia. New York, NY, USA: Association for Computing Machinery; 2007, p. 171–8. http://dx.doi.org/10.1145/1321261.1321292.
[16] Jakob W, d'Eon E, Jakob O, Marschner S. A comprehensive framework for rendering layered materials. ACM Trans Graph 2014;33(4). http://dx.doi.org/10.1145/2601097.2601139.
[17] Stam J. Diffraction shaders. In: Proceedings of SIGGRAPH 99. ACM; 1999, p. 101–10. http://dx.doi.org/10.1145/311535.311546.
[18] Dhillon D, Teyssier J, Single M, Gaponenko I, Milinkovitch M, Zwicker M. Interactive diffraction from biological nanostructures. Comput. Graph. Forum 2014;33(8):177–88. http://dx.doi.org/10.1111/cgf.12425.
[19] Belcour L, Barla P. A practical extension to microfacet theory for the modeling of varying iridescence. ACM Trans Graph 2017;36(4):65:1–65:14. http://dx.doi.org/10.1145/3072959.3073620.
[20] Zinke A, Weber A. Light scattering from filaments. IEEE Trans Vis Comput Graphics 2007;13(2):342–56. http://dx.doi.org/10.1109/TVCG.2007.43.
[21] Marschner SR, Jensen HW, Cammarano M, Worley S, Hanrahan P. Light scattering from human hair fibers. In: ACM SIGGRAPH 2003 Papers. New York, NY, USA: ACM; 2003, p. 780–91. http://dx.doi.org/10.1145/1201775.882345.
[22] Khungurn P, Marschner S. Azimuthal scattering from elliptical hair fibers. ACM Trans Graph 2017;36(2):13:1–23. http://dx.doi.org/10.1145/2998578.

[23] Moon JT, Walter B, Marschner S. Efficient multiple scattering in hair using spherical harmonics. In: ACM SIGGRAPH 2008 Papers. New York, NY, USA: ACM; 2008, p. 31:1–7. http://dx.doi.org/10.1145/1399504.1360630.
[24] Yan L-Q, Tseng C-W, Jensen HW, Ramamoorthi R. Physically-accurate fur reflectance: Modeling, measurement and rendering. ACM Trans Graph 2015;34(6):185:1–185:13. http://dx.doi.org/10.1145/2816795.2818080.
[25] d'Eon E, Francois G, Hill M, Letteri J, Aubry J-M. An energy-conserving hair reflectance model. In: Proceedings of the twenty-second eurographics conference on rendering. Goslar, DEU: Eurographics Association; 2011, p. 1181–7. http://dx.doi.org/10.1111/j.1467-8659.2011.01976.x.
[26] Pekelis L, Hery C, Villemin R, Ling J. A data-driven light scattering model for hair. Pixar Technical Memo 2015;02.
[27] Karis B. Physically based hair shading in unreal. In: SIGGRAPH 2016 course notes; 2016.
[28] Haapaoja R, Genzwürker C. Mesh-driven generation and animation of groomed feathers. In: ACM SIGGRAPH 2019 talks. New York, NY, USA: Association for Computing Machinery; 2019, http://dx.doi.org/10.1145/3306307.3328178.
[29] Chandler AC. A study of the structure of feathers, with reference to their taxonomic significance, v.13:no.11 (1916). Berkeley, University of California Press; 1916, p. 270, URL https://www.biodiversitylibrary.org/item/51770.
[30] Voitkevich A. The Feathers and Plumage of Birds. October House; 1966.
[31] Thompson M. Everything you need to know about feathers. 2014, https://academy.allaboutbirds.org/feathers-article/ [Accessed 7 August 2020].
[32] Stoddard MC, Prum RO. How colorful are birds? Evolution of the avian plumage color gamut. Behavioral Ecology 2011;22(5):1042–52. http://dx.doi.org/10.1093/beheco/arr088.
[33] Doucet S, Shawkey M, Hill G, Montgomerie R. Iridescent plumage in satin bowerbirds: Structure, mechanisms and nanostructural predictors of individual variation in colour. J Exp Biol 2006;209:380–90. http://dx.doi.org/10.1242/jeb.01988.
[34] Babarovic F, Puttick M, Zaher M, Learmonth E, Gallimore E, Smithwick F, Mayr G, Vinther J. Characterization of melanosomes involved in the production of non-iridescent structural feather colours and their detection in the fossil record. J R Soc Interface 2019;16(155):1–9. http://dx.doi.org/10.1098/rsif.2018.0921.
[35] Harvey TA, Bostwick KS, Marschner S. Directional reflectance and milli-scale feather morphology of the African Emerald Cuckoo, Chrysococcyx cupreus. J R Soc Interface 2013. http://dx.doi.org/10.1098/rsif.2013.0391.
[36] Durrer H. Schillerfarben der vogelfeder als evolutionsproblem. Denkschr Schweiz Naturforsch Ges 1977;91:1–127.
[37] Sosa J, Parra J, Stavenga D, Giraldo M. Sexual dichromatism of the blue-throated starfrontlet, coeligena helianthea, hummingbird plumage. J Ornithology 2019. http://dx.doi.org/10.1007/s10336-019-01709-z.
[38] Stavenga D, Leertouwer H, Marshall N, Osorio D. Dramatic color changes in a bird of paradise caused by uniquely structured breast feather barbules. Proc Biol Sci R Soc 2011;278:2098–104. http://dx.doi.org/10.1098/rspb.2010.2293.
[39] Shawkey MD, D'Alba L, Xiao M, Schutte M, Buchholz R. Ontogeny of an iridescent nanostructure composed of hollow melanosomes. J Morphology 2015;276(4):378–84. http://dx.doi.org/10.1002/jmor.20347.
[40] Maia R, Macedo R, D. Shawkey M. Nanostructural self-assembly of iridescent barbules through depletion attraction of melanosomes during keratinization. J R Soc Interface 2011;9:734–43.
[41] Vinther J, Briggs DE, Prum RO, Saranathan V. The colour of fossil feathers. Biol Lett 2008;4(5):522–5. http://dx.doi.org/10.1098/rsbl.2008.0302.
[42] Vinther J, Briggs DE, Clarke J, Mayr G, Prum RO. Structural coloration in a fossil feather. Biol Lett 2009. http://dx.doi.org/10.1098/rsbl.2009.0524, URL http://rsbl.royalsocietypublishing.org/content/early/2009/08/20/rsbl.2009.0524.
[43] Pickrell J. Flying dinosaurs: how fearsome reptiles became birds. Columbia University Press; 2014.
[44] Nordén KK, Faber J, Babarović F, Stubbs TL, Selly T, Schiffbauer JD, Štefanić PP, Mayr G, Smithwick F, Vinther J. Melanosome diversity and convergence in the evolution of iridescent avian feathers – implications for paleocolor reconstruction. Evolution 2018.
[45] Chiang MJ-Y, Bitterli B, Tappan C, Burley B. A practical and controllable hair and fur model for production path tracing. In: ACM SIGGRAPH 2015 talks. New York, NY, USA: Association for Computing Machinery; 2015, http://dx.doi.org/10.1145/2775280.2792559.
[46] Hery C, Villemin R, Ling J. Pixar's foundation for materials. In: SIGGRAPH 2017 Course Notes; 2017.
[47] Jakob W, Arbree A, Moon JT, Bala K, Marschner S. A radiative transfer framework for rendering materials with anisotropic structure. In: ACM SIGGRAPH 2010 Papers. New York, NY, USA: Association for Computing Machinery; 2010, http://dx.doi.org/10.1145/1833349.1778790.
[48] Zhao S, Jakob W, Marschner S, Bala K. Building volumetric appearance models of fabric using micro CT imaging. ACM Trans Graph 2011;30(4). http://dx.doi.org/10.1145/2010324.1964939.
[49] Chen Y, Xu Y, Guo B, Shum H-Y. Modeling and rendering of realistic feathers. In: Proceedings of the 29th annual conference on computer graphics and interactive techniques. New York, NY, USA: ACM; 2002, p. 630–6. http://dx.doi.org/10.1145/566570.566628.
[50] Dana KJ, van Ginneken B, Nayar SK, Koenderink JJ. Reflectance and texture of real-world surfaces. ACM Trans Graph 1999;18(1):1–34. http://dx.doi.org/10.1145/300776.300778.
[51] Baron J, Patterson E. Procedurally generating biologically driven feathers. In: Lecture notes in computer science, Springer; 2019.
[52] Robertson B. In fine feather. Computer Graphics World 2010. URL http://www.cgw.com/Publications/CGW/2010/Volume-33-Issue-9-October-2010-/In-Fine-Feather.aspx [Accessed 1 November 2018].
[53] Harvey TA. Spatially- and directionally-varying reflectance of milli-scale feather morphology. [Ph.D. thesis], ECommons, Cornell's Digital Library; 2012, p. 150.
[54] Koch SL, Shriver MD, Jablonski NG. Variation in human hair ultrastructure among three biogeographic populations. J Struct Biol 2019;205(1):60–6. http://dx.doi.org/10.1016/j.jsb.2018.11.008, URL http://www.sciencedirect.com/science/article/pii/S1047847718303083.
[55] Christensen P, Fong J, Shade J, Wooten W, Schubert B, Kensler A, Friedman S, Kilpatrick C, Ramshaw C, Bannister M, Rayner B, Brouillat J, Liani M. RenderMan: An advanced path-tracing architecture for movie rendering. ACM Trans Graph 2018;37(3). http://dx.doi.org/10.1145/3182162.